Food Chemistry 395 (2022) 133577

Contents lists available at ScienceDirect

Food Chemistry

journal homepage: www.elsevier.com/locate/foodchem

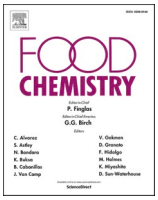

A comparative study of S-nitrosylated myofibrillar proteins between red, firm and non-exudative (RFN) and pale, soft and exudative (PSE) pork by iodoTMT-based proteomics assay

Rui Liu [a,b], Keyue Li [a], Guoyue Wu [a], Man Qin [a], Hai Yu [a], Mangang Wu [a], Qingfeng Ge [a], Shenglong Wu [b,*], Wenbin Bao [b], Wangang Zhang [c,*]

[a] School of Food Science and Engineering, Yangzhou University, Industrial Engineering Center for Huaiyang Cuisin of Jiangsu Province, Yangzhou, Jiangsu 225127, China
[b] Jiangsu Key Laboratory of Animal Genetic Breeding and Molecular Design, College of Animal Science and Technology, Yangzhou University, Yangzhou 225009, China
[c] College of Food Science and Technology, Nanjing Agricultural University, Nanjing 210095, China

ARTICLE INFO

Keywords:
PSE meat
RFN meat
Myofibrillar protein
S-nitrosylation
Proteomics

ABSTRACT

In this paper, the S-nitrosylated myofibrillar protein in pork was comparatively analyzed between pale, soft, and exudative (PSE) and red, firm, and non-exudative (RFN) meat. The S-nitrosothiol and immunoblot of S-nitrosylated protein indicated that the overall protein S-nitrosylation level in PSE pork was higher than that in RFN pork. Proteomics showed that 114 SNO-modified cysteines corresponding to 65 proteins were over-expressed in PSE samples while 74 nitrosylated cysteines of 20 proteins were over-expressed in RFN samples. Differential proteins including myosin, actin, actinin, nebulin, titin, troponin-I, and filamin were distributed in the cytoskeleton and muscle fibers, participating in muscle contraction, cell development, and myofibril assembly by exerting binding activity. The enriched KEGG pathways included tight junction, regulation of actin cytoskeleton, glycolysis/gluconeogenesis, AMPK signaling pathway, and HIF-1 signaling pathway. Our data suggest that S-nitrosylation of myofibrillar protein could be an alternative pathway of NO involved in the regulation of fresh meat quality.

1. Introduction

Desired quality of pork meat by consumer is typically red, firm and non-exudative (RFN) while pale, soft and exudative (PSE) pork is a defective meat, which has been a challenge for the development of global pork meat industry. Many factors contribute to the formation of PSE pork, including animal genetics, nutrition, pre-slaughter stress, and carcass processing and storage conditions (Barbut et al., 2008). PSE pork is exhibited with the characteristics of pale meat color, soft texture, high juice exudation rate, which reduces the consumers' purchasing desire (Karamucki, Jakubowska, Rybarczyk, & Gardzielewska, 2013). On the other hand, the protein in PSE meat is denatured to some extent, resulting in poor processing capacity and huge economic losses of pork meat industry. The primary cause of PSE meat has been known as the rapid and excessive glycolysis accompanying with low pH-induced protein denaturation of postmortem meat at high temperature (Barbut et al., 2008; Huff-Lonergan & Lonergan, 2005). However, the molecular mechanism of biochemical changes in PSE meat during the postmortem aging has not been fully elucidated and still needs further investigation.

It is well-known that the extent of muscle contraction in rigor mortis and the integrity of muscle structure during postmortem aging are crucial factors in affecting the meat quality. Proteolysis of those proteins including actin, myosin, troponin, tropomyosin, titin, desmin and nebulin contributes for the disruption of the myofibril architecture during the conversion of muscle to meat process (Lana & Zolla, 2016). In addition, many proteomics studies have revealed that those proteins have been identified to be differentially expressed in postmortem meat and affected by variable factors, such as breed, gender, rearing practices, and muscle types (Picard, Gagaoua & Hollung, 2017). Some proteins can be adopted as candidate biomarkers and associated with meat quality traits, which gains a better understanding of molecular mechanism involved in formation of meat quality. As summarized by Picard et al. (2017), however, the correlation between candidate biomarkers and meat quality traits exhibited inconsistence among studies. For example,

* Corresponding authors.
E-mail addresses: slwu@yzu.edu.cn (S. Wu), wangang.zhang@njau.edu.cn (W. Zhang).

https://doi.org/10.1016/j.foodchem.2022.133577
Received 17 February 2022; Received in revised form 21 June 2022; Accepted 23 June 2022
Available online 25 June 2022

actin was identified to be positively correlated with meat shear force in the study of Hwang, Park, Kim, Cho and Lee (2005), but negative correlation was shown as reported by Lametsch et al. (2003). Moreover, a potential protein marker was determined with different molecular weight and isoelectric point in one study as a consequence of different isoforms, degraded fragments and post-translation modification (Hwang et al., 2005). This may confound the basic protein expression and exaggerate the relationship with meat quality. Thus, the status of protein in postmortem meat, in particular, post-translation modifications which are able to change protein localization, activity and function, is recommended to be addressed for robustly predicting meat quality traits.

Protein S-nitrosylation, which refers to the covalent attachment of nitric oxide (NO) group to the sulfhydryl of protein cysteine to form S-nitrosothiol, is considered as a common post-translational modification in cell signaling pathway (Hess, Matsumoto, Kim, Marshall, & Stamler, 2005). Previous researches have been conducted to investigate the potential role of NO and its-induced protein S-nitrosylation in regulating fresh meat quality by managing the content of NO in postmortem muscle (Cottrell, McDonagh, Dunshea, & Warner, 2008; Cottrell, Ponnampalam, Dunshea, & Warner, 2015). A hypothesis was made that NO produced in postmortem muscle would modify the protein cysteine for S-nitrosylation, which may regulate the protein activity, function and interaction, and in turn affect physiological metabolism of muscle and the meat quality during postmortem aging (Liu, Warner, Zhou & Zhang, 2018a). Research was progressed by the finding of a vast of S-nitrosylated proteins belongs to glycolytic enzymes, calcium channel proteins, heat shock proteins, and antioxidant enzymes in aging samples of pork longissimus thoracis muscle (Liu et al., 2018b). Wang et al. (2019), Wang et al. (2020) further determined the differential protein S-nitrosylation level of glycogen phosphorylase (GP), phosphofructokinase (PFK) and pyruvate kinase (PK), ryanodine receptor 1 (RyR1) and sarcoplasmic reticulum calcium ATPase 1 (SERCA1) between PSE and RFN pork, deciphering the PSE meat formation from the perspective of protein S-nitrosylation effect on glycolysis and cytoplasmic calcium. However, the literature was shown that many myofibrillar proteins such as myosin, actin, desmin, myosin and troponin *in vivo* can undergo S-nitrosylation modification in skeletal muscle (Su et al., 2013). The biological function of skeletal muscle was reported to be regulated by NO and protein S-nitrosylation, including muscle contraction and muscle cell differentiation (Stamler & Meissner, 2001). The myofibrillar proteins sensitive to S-nitrosylation were found to decrease the sensitivity of myofilaments to calcium ions (Figueiredo-Freitas et al., 2015). Many cytoskeletal proteins and the adhesion proteins were identified as nitrosoproteins, indicating the S-nitrosylation of protein might be an alternative pathway for NO to modulate muscle contractile function and activity. Thus far, knowledge on myofibrillar protein S-nitrosylation in postmortem muscle and its possible relationship with pork meat quality are still lacked. The objective of this paper was to characterize myofibrillar protein nitrosylation and identify their specific S-nitrocysteine sites in PSE meat compared to the RFN meat, and gained a better understanding about the involvement of NO and protein S-nitrosylation during the process of muscle to meat conversion.

2. Materials and methods

2.1. Pork samples collection

Pigs (Castrated Duroc × Landrace × Yorkshire crossbred pigs, 100 ± 10 kg) were slaughtered at a commercial meat processing plant (Sushi Meat Co., Ltd., Huai'an, Jiangsu, China) following the Ordinance on Pig Slaughtering Management in China (GB/T 17236-2019) (Wang et al., 2021). The pigs were electrically stunned and the carcasses were randomly selected by measuring the pH_{1h} of *longissimus thoracis* (LT) at the 3rd to 4th rib to screen out possible PSE ($pH < 5.8$) and possible RFN ($pH > 6.0$) meat at the slaughtering line, each with 10 pig carcasses (Chmiel, Słowiński, & Janakowski, 2014). Then, the LT muscles from 3rd and 13th rib were removed from the right half of each carcass. Each loin was cut into 2 chops with approximately equal size and weight, and the anterior part was assigned as 1 h and the posterior part was assigned as 24 h postmortem treatment. Each chop was weighted and the samples of 1 h post-slaughter were directly delivered for color measurement and preparation of biochemical samples. Chops assigning as 24 h postmortem treatment were individually vacuum-packed and stored at 4 °C for pH, color and purge loss measurements. A portion of 50 g LT muscle of each treatment was minced to be frozen in liquid nitrogen and stored at −80 °C for further biochemical sample preparation. Finally, the PSE samples (n = 8) and RFN samples (n = 8) were obtained according to the criteria developed Warner, Kauffman, & Greaser (1997) with a slight modification: PSE meat, $pH_{24h} < 5.5$, $L^*_{24h} > 50$, and purge $loss_{24h} > 5\%$, RFN meat, $5.5 < pH_{24h} < 5.8$, $42 < L^*_{24h} < 50$, purge $loss_{24h} < 5\%$.

2.2. pH, color, and purge loss determinations

The pH of LT muscle was determined by using a portable pH meter (Testo 205, Germany) attached with a glass electrode. The standardized buffer solutions (pH 4.00 and 7.00, BBI Life Sciences, Shanghai, China) were used for the pH meter calibration before each measuring. At 1 h postmortem, the pH meter was calibrated at room temperature (25℃) and the LT muscle of pig carcass at the processing line was approximately 35℃. At 24 h postmortem, the standardized buffer solutions were placed in the refrigerator (4℃), which was same as the meat samples. pH was recorded once the digital display of pH meter was stable after the electrode penetrated into the meat. pH values in four different sites of each meat chop were measured and those four repeated measurements of pH value were averaged for statistical analysis. The instrumental color parameters were measured with the colorimeter of a D65 light source, 8 mm measurement aperture, and 2° observation angle (CR-400, Konica Minolta, Japan). Each meat sample was placed on the plate to be exposed to air for 10 min at room temperature (25℃) before measurements. The colorimeter was calibrated with a standard white plate each time before measuring. The L^*, a^* and b^* values of the meat samples were calculated by averaging values of three different points of meat surface. Purge loss was measured by recording the initial weight of LT before vacuum packing and the weight after storing 24 h at 4 °C, in which the exudate was removed and surface liquid was wiped dry with filter paper. Purge loss was calculated as percentage of the weight loss over the initial weight of each sample.

2.3. Detection of nitric oxide synthase (NOS) activity

NOS activity was determined by a commercial NOS detection kit (Jiancheng Bioengineering, Inc., Nanjing, China). Protein sample was prepared by homogenizing 0.5 g of well-minced LT muscle with extraction buffer (25 mM Tris − HCl, 1 mM ethylenediaminetetraacetic acid (EDTA), and 1 mM ethylene glycol-bis(β-aminoethyl ether)-N,N,N′, N′-tetraacetic acid (EGTA, pH 7.4). The homogenate was then centrifuged at 20,000 g for 15 min at 4 ℃. The supernatant was obtained and used for the detection of NOS activity. Protein concentration was detected by a Pierce BCA Protein Assay kit (Thermo Fisher Scientific, IL, USA). NOS activity was expressed as the nmoles per min per milligram protein.

2.4. Preparation of myofibrillar protein

The well-chopped LT muscle (0.5 g) was homogenized twice at 4 °C with 4.5 mL pre-cooled phosphate buffer (0.1 M NaCl, 10 mM $Na_2HPO_4{\cdot}12H_2O$, 2 mM $MgCl_2{\cdot}6H_2O$ and 1 mM EGTA at pH 7.0), and 15 s each time with a 30 s interval between bursts. The homogenate was then centrifuged at 2,000 g for 15 min at 4 °C and supernatant was slowly decanted. Then, precipitate was washed twice with 4.5 mL of the phosphate solution and three times with 4.5 mL of 0.1 M NaCl. The precipitate of the centrifuged sample was collected as myofibrillar

protein fraction. Protein concentration was measured with BCA Protein Assay kit and adjusted to 4 mg/mL with HENS buffer (100 mM HEPES, pH 7.8, 1 mM EDTA, 0.1 mM Neocuproine, and 1% SDS (w/w)) for further protein S-nitrosylation detection.

2.5. S-nitrosothiol (SNO) detection

Total protein SNO amount in the sample was determined by Saville method with reference to Liu et al. (2018b). Briefly, two aliquots of 50 μL myofibrillar protein sample or S-nitrosoglutathione (GSNO) standard samples were mixed with reagent A (1% sulfanilamide, 0.5 M hydrochloric acid) or reagent B (0.2% mercuric chloride, 1% sulfanilamide, and 0.5 M hydrochloric acid) in a 96-well plate, respectively. After reacting at 25℃ for 5 min at room temperature, 100 μL of reagent C (0.5 M hydrochloric acid, 0.02% N-1-naphthyl ethylenediamine) were also added and then oscillated for 30 s in a microplate reader (IN FINITE 200 PRO, Tecan Trading AG, Switzerland). After reacting at 25℃ for 5 min, absorbance was detected at 540 nm. The linear range of GSNO concentration was set as 3.125–200 μM for making the standard curve with the absorbance difference between group B and group A. SNO concentration of myofibrillar protein sample was determined by using the GSNO standard curve and expressed as μM/mg protein.

2.6. Biotin switch method

Myofibrillar protein samples for the S-nitrosylation detection were prepared by the biotin switch method (Zhu et al., 2021). Myofibrillar protein concentration was adjusted to 2 mg/mL by HENS buffer and then 700 μL samples were removed into a new tube. Five-fold of pre-cooled acetone (v/v, −20 °C) was added and then precipitated at −20 °C for 12 h. Sample was then centrifuged at 10,000 g for 10 min at 4 °C, and the acetone was gently discarded. Sample was then air-dried at 25℃ for 10 min. For blocking the free sulfydryl, 70 μL of 1 M methyl thiosulfonate (MMTS) were added, vigorously vortexed for 1 min and incubated for 30 min at 25℃. After the incubation, protein was also precipitated twice with pre-cooled acetone to remove excess MMTS. The dried protein pellet was dissolved in 700 μL HENS solution, followed by the sequential addition of 14 μL of IodoTMT labeling agent (0.2 mg IodoTMTsixplex in 20 μL of dimethylsulfoxide, 90100, Thermo Fisher Scientific, IL, USA) and 28 μL of 1 M sodium ascorbate. The mixture was severely vortexed and the reaction for SNO reduction and labeling was performed in dark at 37 °C for 1 h. After the reaction was completed, one aliquot of 50 μL of protein sample was combined with 2 × loading buffer (100 mM Tris-HCl, 20% glycerol (w/w), 4% SDS (w/w), 0.05% bromophenol blue (v/v) and 5% β-mercaptoethanol (v/v)) at a ratio of 1: 1, followed by 10 min incubation in a 95 °C water bath for making electrophoretic samples. The remaining aliquot of protein sample solution was added with dithiothreitol (DTT, 1 M) to terminate the labeling reaction, and the excess labeling reagent was removed by the precipitation with pre-cooled acetone at −20 °C as described above. Myofibrillar protein was re-dissolved with HENS buffer, subsequently added with 100 μL of iodoacetamide and incubated at 37 °C for 1 h in dark. By performing the acetone precipitation at −20 °C, protein was collected and stored at −80 °C for S-nitrosylation detection by LC-MS/MS analysis.

2.7. Detection of S-nitrosylated myofibrillar protein by western blotting

A dose of 10 μg myofibrillar protein sample was loaded onto the polyacrylamide gel comprising of 4% stacking gel and 10% separating gel. Gels were run on a Bio-Rad Mini-Protean II electrophoresis unit (Bio-Rad Laboratories, Hercules, CA) at 90 V for 30 min, and then at 120 V for 60 min until the dye front reached the bottom of the gel. After electrophoresis, myofibrillar protein was transferred into polyvinylidene difluoride (PVDF) membranes setting at 90 V for 90 min at 4 °C. Then, the membrane was blocked with 5% (w/v) non-fat dry milk in TBST buffer (20 mM Tris-base, 137 mM NaCl, 5 mM KCl and 0.05% (v/v) Tween-20) at room temperature for 2 h. After discarding the blocking solution, membrane was incubated with the anti-tandem mass tag (TMT) antibody (S-nitrosylation western blot assay kit, Thermo Fisher Scientific, USA) at dilution of 1: 1,000 at 4 °C for 12 h. The membrane was washed with TBST solution for three times (10 min/wash). After incubated with the secondary antibody of horseradish peroxidase (HRP) -labeled sheep anti-mouse immunoglobulin (BS12478, Bioworld, USA) at dilution of 1: 100,000 for 2 h at room temperature, the membrane was washed with TBST again. Finally, PVDF membrane was treated with BeyoECL Moon buffer (Beyotime Institute of Biotechnology, Haimen, China), and reacted for 90 s and manually exposed to X-Ray in dark. The X-Ray film was scanned with an Epson perfection V30 SE scanner (Epson, Nagano, Japan). The membrane with chemiluminescence was removed to detect β-actin, which was considered as an internal standard, by stepwise washing with distilled water for 5 min, antibodies removal buffer (Beyotime Institute of Biotechnology, Haimen, China) for 10 min and 4 times of TBST buffer for 20 min. The rabbit polyclonal anti-β-actin antibody (I102, Bioworld, USA) was used as the primary antibody at the dilution of 1: 20,000 with TBST buffer and HRP-labeled goat anti-rabbit immunoglobulin (BS13278, Bioworld, USA) was regarded as the secondary antibody with a dilution of 1: 100,000. The protein band densities were analyzed with the Quantity one software (Version 4.6.2, Bio-Rad, USA).

2.8. LC-MS/MS analysis

The myofibrillar protein pellet prepared by BSM was solubilized in 12 mL of 50 mM NH_4HCO_3. The enzymolysis of protein was performed by adding 160 μL of 0.08 μg/μL trypsin and incubated at 37℃ for 12 h. The resulting peptides were desalted by polypeptide desalting centrifugal column (89852, Thermo Fisher Scientific, IL, USA) and then vacuum lyophilized. Lyophilized peptide was redissolved with TBS buffer (20 mM Tris-base, 137 mM NaCl, 5 mM KCl) and the enrichment was done by adding 400 μL of anti-TMT resin for 2 h incubation at room temperature. The unbound peptides were subsequently washed with a column volume of 2 M urea in TBS buffer, TBS buffer, and ultrapure water, each for 4 times. The enriched peptides were eluted by the TMT elution buffer (90104, Thermo Fisher Scientific, IL, USA). Sample was then desalted, vacuum lyophilized and dissolved in 20 μL of 2% acetonitrile with 0.1% formic acid.

Liquid chromatography-mass spectrometry (NanoLC-MS/MS) was performed with the Easy nLC 1200 system for chromatographic separation. The peptide sample of 2 μg was injected at a nanoliter flow rate. The peptide separation was conducted by using a gradient mobile phase of solution A (0.1% formic acid) and solution B (0.1% (v/v) formic acid, and 80% (v/v) acetonitrile) as follows: 95% A for column equilibration, 0–2 min, B from 2% to 4%, 2–110 min, B from 4% to 30%, 110–112 min, B from 30% to 90%, and 112–120 min, 100% B. Spray voltage was set as 2 kV. After the peptide separation, data correlation acquisition (DDA) mass spectrometry was performed on a Q Exactive HF-X compound quadrupole-orbital trap mass spectrometer equipped with a nano electrospray ion source (nESI). The parameters for MS1 scanning were set as follows: the scanning range of parent ion was 350–1800 *m/z*, the resolution was 60,000 (*m/z*: 200), the automatic gain control (AGC) target was 3×10^6, the maximum injection time (IT) was 50 ms, and the number of micro-scans was set to 1. The 15 highest intensity precursor ions were selected from each MS1 scan for high energy collision dissociation (HCD). In the MS2 scan, the resolution was 15,000 (*m/z*: 200), the AGC target was 1×10^5, the maximum IT was 50 ms, the intensity threshold was 2×10^4, the isolation window was 1.6 *m/z*, and the normalized collision energy was 32. The number of micro-scans was set to 1, and the dynamic exclusion time for peptide scans was 30 s.

The original files were imported into the Proteome Discoverer Software (Version 2.4, Thermo Fisher Scientific, IL, USA) for database retrieval against the database Uniprot-Sus scrofa_122027_202008. The

enzyme was set to trypsin and the maximum allowed number of missed cleavage sites was set to 2. The main search segment tolerance, first search segment tolerance, and MS/MS tolerance were set to 4.5 ppm, 20 ppm, and 20 ppm, respectively. The peptide map-matching FDR and the protein FDR were both set to ≤0.01, and the variable modifications included iodoTMT6 modification, oxidative modification, and protein *N*-terminal acetylation.

2.9. Bioinformatics analysis

The S-nitrosylated proteins differently detected between PSE and RFN group were selected based on fold change (FC) > 1.30 or <0.77 (PSE meat vs RFN meat) and $P < 0.05$ was identified. Those differential proteins were used for the significance enrichment analysis by the gene ontology (GO) (https://geneontology.org/) annotation in which the protein enrichment significance level for a given GO term was tested by Fisher's Exact Test. The Kyoto Encyclopedia of Genes and Genomes (KEGG) (https://www.genome.jp/kegg/) pathway enrichment analysis was performed. Significant protein enrichment levels for each pathway, in units of the KEGG pathway, were obtained by the Fisher's Exact Test to identify significant metabolic and signal transduction pathways. The protein–protein interaction (PPI) network was derived from the Omicsbean system (https://www.omicsbean.cn).

2.10. Statistical analysis

Significant differences between RFN meat and PSE meat samples were analyzed by Paired Samples T-Test with SPSS version 16.0 software (SPSS Inc., Chicago, IL, USA). The level of significance was considered as $P < 0.05$.

3. Results and discussion

3.1. Meat quality

As shown in Table S1, the LT muscles were categorized into PSE and RFN pork based on the differences in pH, color and purge loss during 24 h postmortem aging. PSE meat group presented significantly higher L^* but lower pH than that of RFN meat group at 1 h and 24 h postmortem ($P < 0.05$). Additionally, a lower a^* value combined with a higher b^* value were also observed in PSE meat showing with paleness appearance. Water hold capacity as indicated by purge loss in PSE meat group was significantly lower than that in RFN meat group, implying more water loss of PSE meat during 24 h postmortem aging. The results in the current study are consistent with the previous reports (Wang et al., 2019; Wang et al., 2020) and the classified standard of PSE and RFN pork (Warner et al., 1997).

3.2. NOS activity and SNO content

Endogenous NO in muscle can be formed by NOS catalysis of arginine to citrulline, and NOS activity is the prerequisite for NO production thus playing a role during the aging process of postmortem pork (Liu et al., 2015). The NOS activity and SNO content is shown in Fig. 1a and 1b, respectively. LT muscle presented a decreased NOS activity, and a gradient increase of SNO content during the 24 h of postmortem aging ($P < 0.05$). The NOS activity in PSE pork was significantly lower than that of RFN pork ($P < 0.05$). On the contrary, PSE sample possessed a relatively higher SNO content in comparison to RFN sample ($P < 0.05$). The present study showed higher NOS activity in RFN meat than that in PSE meat group, which is consistent with the report by Wang et al. (2019), where PSE meat presented lower NOS activity than that of the RFN group at 1 h postmortem. Similarly, Brannan & Decker (2002) detected NOS activity in postmortem chicken thigh muscle and found that NOS activity was inhibited by lower pH value. It was suggested that the pH difference in postmortem muscle may affect the NOS activity in PSE and RFN meat. Moreover, post-translational modifications of proteins, including S-nitrosylation, were reported to regulate NOS activity by subcellular targeting. The total SNO content in PSE pork was higher than that in RFN pork, which might cause the variable S-nitrosylation of NOS, resulting in NOS activity difference between PSE and RFN meat samples. The gradual increase of SNO content of myofibrillar proteins during postmortem aging is also in accordance with the previous reports for the sarcoplasmic protein in pork LT muscle (Liu et al., 2018b), indicating the reduced oxidative stability in postmortem meat. NOS activity and protein S-nitrosylation level differed between PSE and RFN pork, suggesting a potential role of NO is involved during the process of muscle to meat conversion (Fig. 2).

3.3. Immunoblot of S-nitrosylated myofibrillar protein

The S-nitrosylated protein bands in LT muscle at 1 h postmortem aging are shown in Fig. 3. The optical density of protein band indicated the extent of protein S-nitrosylation, and the abundance was calculated by the relative intensity of protein bands over that of β-actin (Supplementary Table S2). It was found that the total abundance of S-

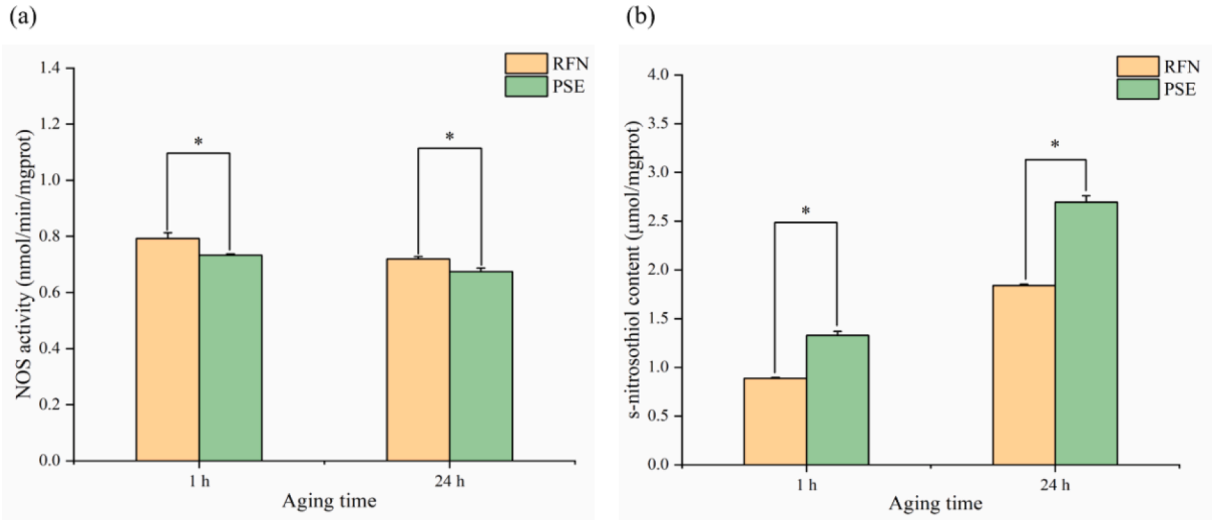

Fig. 1. Nitric oxide synthase (NOS) activity (a) and S-nitrosothiol content (b) at 1 h, 24 h postmortem of red, firm, and non-exudative (RFN) and pale, soft, and exudative (PSE) meat. * indicated significant differences among treatment groups ($P < 0.05$). The bar indicates standard error of mean.

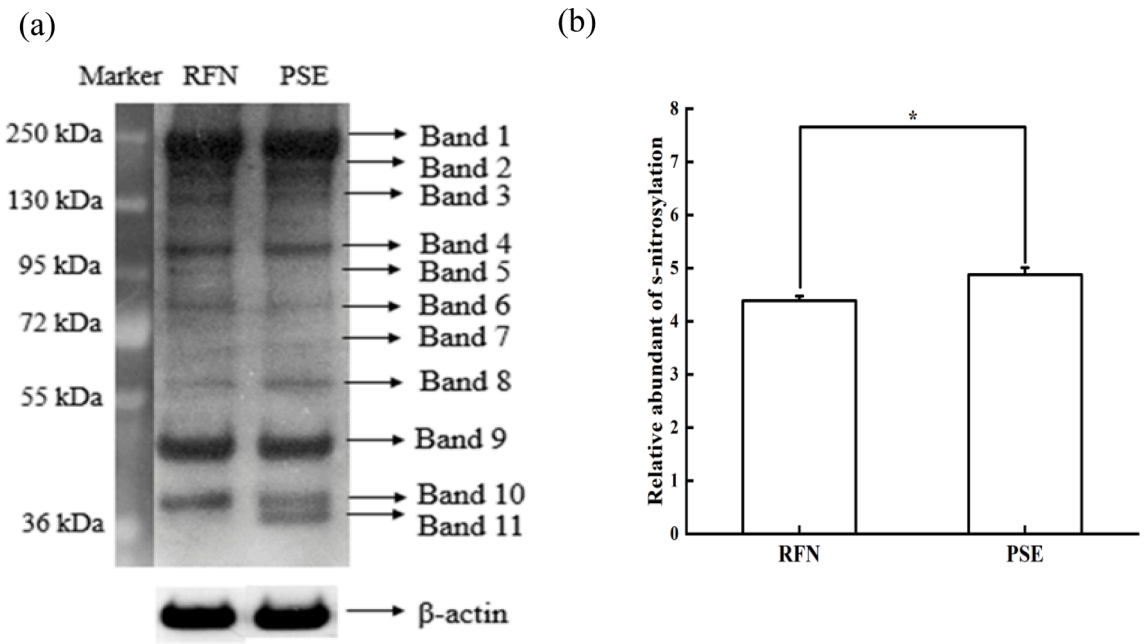

Fig. 2. Comparison of S-nitrosylated protein bands between PSE and RFN meat at 1 d postmortem. (a) Representative image of immunoblotting of S-nitrosylated myofibrillar protein and β-actin. (b) Relative intensity of total S-nitrosylated protein bands. Different letters indicate significant difference between two groups at P < 0.05. The bar indicates standard error of mean.

nitrosylated protein in PSE meat was significantly higher compared to RFN meat ($P < 0.05$, Fig. 3b), whereas individual proteins bands exhibited a high variability. In comparison to RFN pork, PSE pork showed a lower intensity in protein band 1, 6, and 10, while a higher intensity for protein band 8 and 11 (only detected in PSE group). The remaining protein bands showed no significant differences among two groups ($P > 0.05$, Supplementary Table S2). The degree of S-nitrosylation of myofibrillar proteins varied between PSE and RFN groups, implying that NO and its-induced protein S-nitrosylation might be involved in regulating pork meat quality via myofibrillar proteins and its associated pathways.

3.4. Identification and quantification of S-nitrosylated myofibrillar protein

By utilizing the iodoTMT-based proteomisc, a total of 1,247 cysteine sites corresponding to 419 proteins were identified with S-nitrosylation modification in myofibrillar protein fraction of pork LT muscle at 1 h postmortem aging (Fig. 3a). The differential S-nitrosylated proteins and Cys-sites between PSE and RFN pork are presented in Supplementary Table S3. There were 180 SNO-modified Cys-sites in 170 peptides, among which 10 peptides contained two Cys-sites. Compared to RFN meat, PSE meat had 96 up-regulated Cys-sites in 65 corresponding proteins and also 74 down-regulated Cys-sites in 20 proteins (Fig. 3b). The heatmap of PSE and RFN meat samples in triplicate showed a reliable detection of Cys-SNO modification (Fig. 3c). The high variability of individual proteins of S-nitrosylation among two groups was indicated, which accorded with the immunoblotting result of S-nitrosylated protein band detection.

The representatives of differential S-nitrosylated proteins and SNO-modified cysteine sites are shown in Table 1. As expected, cytoskeletal proteins were mostly identified and included myosin, actin, actinin, nebulin, titin, troponin-I, filamin, plectin, microtubule-associated protein and PDZ and LIM domain protein. Myosin isoforms were matched with different abundance of Cys-SNO modification among two groups. Among them, Cys 676, Cys 699 and Cys 1344 in myosin 1 were higher expressed in RFN sample, while Cys 995 in myosin 9 was over-abundance in PSE sample. The S-nitrosylation of Cys-sites in plectin, microtubule-associated protein, PDZ and LIM domain protein 3, and filamin C of the PSE group was higher than those of the RFN group whereas the Cys-SNO modification of actin, nebulin, actinin alpha 3 and troponin I in the PSE group was lower than those of the RFN group. The giant protein titin was detected with multiple cysteines modified by S-nitrosylation. The PSE group showed a higher SNO modification of Cys1976 in titin and Cys 26,581 in titin isoform X6 but lower for Cys1976 in titin and other 39 Cys-sites in titin isoform X6 when compared to RFN group ($P < 0.05$).

Previous studies have been mainly concentrated on S-nitrosylated protein detection of sarcoplasmic protein fractions in skeletal muscle of pig (Liu et al., 2018b), beef (Zhu et al., 2021), and mouse (Su et al., 2013). In the present study, the S-nitrosylation modification of myofibrillar protein Cys-sites in pork postmortem muscle was identified for the first time at a large scale by proteomics. The primary outcome of this study was the findings of myofibrillar fraction of S-nitrosylated proteins, which were the main constituent of muscle fibers. At present, it has been identified that a variety of cytoskeletal proteins was capable to be modified by S-nitrosylation (Horenberg, Houghton, Pandey, Seshadri, & Guilford, 2019). Figueiredo-Freitas et al. (2015) reported that α-actin, myosin light chain 3, myosin heavy chain 6, myosin binding protein C, troponin I, troponin C, titin and α-tropomyosin 1 were shown to be S-nitrosylated in mouse cardiomyocytes. Bansbach & Guilford (2016) identified S-nitrosylated proteins in rat skeletal muscle tissue and found that α-, β- and γ-isoforms of actin underwent significant S-nitrosylation modification.

Myosin and actin are the main components of thick filaments and thin filaments, respectively. The thick and thin filaments cross and slide each other through the interaction between myosin head and actin filaments, which is responsible for muscle contraction (Hartman & Spudich, 2012). Myosin family is a large and diverse protein family, which is involved in many cellular pathways (Woolner & Bement, 2009). In this study, three myosin isoforms were identified to be modified by S-nitrosylation, among which Cys995 of myosin-9 was expressed higher in the PSE group, while other four Cys-sites in myosin-1 were over-expressed in RFN group ($P < 0.05$). Similarly, Evangelista et al. (2010) found that both myosin heavy chain in rats and myocardial cell in humans were modified by S-nitrosylation. It was revealed that the S-

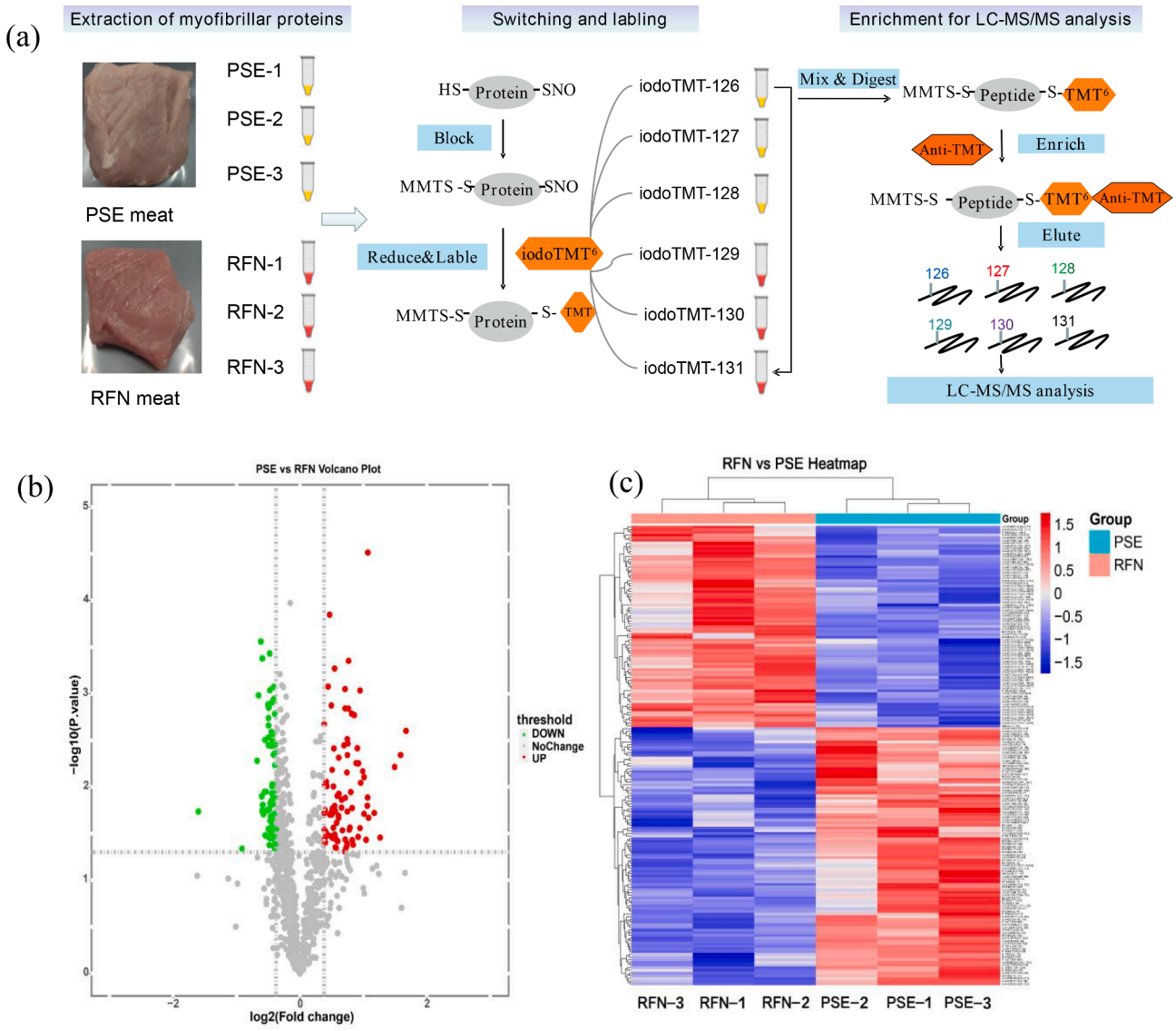

Fig. 3. Proteomics identification of S-nitrosylated proteins of PSE and RFN meat at 1 d postmortem. (a) Schematic workflow of modified switch method coupled with iodo tandem mass tag to identify S-nitrosylated proteins of two groups. (b) Volcano plot of the differential proteins of S-nitrosylation between PSE and RFN mea. (c) Heatmap of the differential proteins between PSE and RFN meat.

nitrosylation of myosin could change the hydrolysis cycle of myosin, reduce the movement speed of actin, and enhance the isometric contraction force of the muscle, thus affecting the muscle contraction (Evangelista et al., 2010; Horenberg et al., 2019). In addition, α-actin was reported to be SNO-modified *in vivo* and *in vitro* (Bizzozero & Zheng, 2009; Chen et al., 2008). This study showed that Cys287 of α-actin was modified by S-nitrosylation. Likewise, Figueiredo-Freitas et al. (2015) also detected S-nitrosylation modification of actin at Cys287 in smooth muscle of mice. *In vitro* S-nitrosylation of β-actin with NO donor GSNO revealed a slight decrease in the monomer polymerization capacity of actin and an increased time for binding myosin during its hydrolysis (Bansbach & Guilford, 2016). The different degree of SNO-modification in myosin-1 and α-actin between PSE and RFN meat was putative to affect the sliding and crossing between thick and thin filaments when the postmortem muscle was developed into rigor mortis. The speed and extent of bounding of actin to myosin is critical to the muscle contraction and meat quality change in postmortem meat, however, the S-nitrosylation effect is unknown and needs to be further studied.

Titin can maintain the integrity of sarcomere structure and stabilize the center of the thick filament between the Z-disks (Huff-Lonergan, Zhang, Lonergan, 2010; Linke & Hamdani, 2014). In this study, S-nitrosylation modification was detected in titin isoform X6 with multiple Cys-sites. It has been reported that S-nitrosylated titin was associated with reduced calcium sensitivity (Figueiredo-Freitas et al., 2015) and was thought to have an effect on the titin components of the passive stiffness of the sarcomere (Mayans, Wuerges, Canela, Gautel, & Wilmanns, 2001). Besides, S-nitrosylation modifications of myosin-binding protein C, troponin I and troponin C were also reported to relate with the decreased calcium sensitivity (Figueiredo-Freitas et al., 2015). Those proteins were also detected with undergoing S-nitrosylated modification in the current study, among which myosin binding protein C and troponin *C*2 were matched as uncharacterized protein due to the deficiency of pig protein data bank (Supplementary Table S1). Wang et al. (2019) reported that the sarcoplasmic calcium concentration in PSE meat was 5.8 fold higher than that in RFN meat at 1 h postmortem. It is suggested that the S-nitrosylation might affect the extent of muscle contraction by affecting the calcium sensitivity with variable calcium concentrations at the early stage of postmortem aging. Plectin, a high-molecular-weight cytoskeletal junction protein, is connected to actin and microtubule network and is anchored to the subcapsular skeleton

Table 1
Representative candidates of differential S-nitrosylated proteins and SNO-modified cysteine sites identified from myofibrillar protein fraction of pork LT muscle between PSE meat and RFN meat.

No.	Protein names	Accessions	Annotated Sequence	Cys-sites	FC	*P*.value
1	Myosin-1	Q9TV61	[RK].HDCDLLR.[E]	1344	0.72	**
			[R].CNGVLEGIR.[I]	699	0.75	**
			[R].CIIPNETK.[TS]	676	0.74	**
2	Myosin-1 isoform X1	A0A481AX92	[R].RESIFCIQYNIR.[A]	817	0.66	*
3	Myosin-9	A0A480QL86	[K].LEEDQIIMEDQNCK.[L]	995	1.47	*
4	Actin, alpha skeletal muscle	A0A481CYB2	[RK].CDIDIRK.[D]	287	0.72	*
5	Actinin alpha 3	A0A5G2RET9	[K].DGLALCALIHR.[H]	195	0.75	*
6	Filamin C	F1SMN5	[R].VGVTEGCDPTR.[V]	1349	1.68	**
			[R].SPFPVHVAEACNPNACR.[A]	478	1.32	*
			[R].VHTPSGAVEECYVSELDSDK.[H]	2449	1.64	**
7	Plectin	A0A287B217	[K].GDECQMVGPAQPFHWK.[V]	797	1.64	*
8	Nebulin	F1SHX0	[K].KCQTLVSDIDYR.[N]	3824	0.73	*
			[R].NYLHQWTCLPDQHDVIQAR.[K]	4084	0.70	*
9	Titin	A0A480J3J1	[R].VVGKPDPECEWYKNGVK.[I]	1976	1.38	**
			[K].NCAVVDESVYGFK.[L]	2636	0.67	*
10	Troponin I	B3VI70	[K].HKVCMDLR.[A]	134	0.76	*
11	PDZ and LIM domain protein 3	Q6QGC0	[K].MPLCDK.[C]	135	1.71	*
			[R].SSGCSTPSGIDGGSGR.[S]	62	1.46	*
12	Microtubule-associated protein	A0A287AY86	[K].CPWGDR.[E]	1153	1.77	*
13	Glyceraldehyde-3-phosphate dehydrogenase	P00355	[R].VPTPNVSVVDLTCR.[L]	245	1.67	*
			[K].IVSNASCTTNCLAPLAK.[V]	150;154	1.59	*
14	Phosphoglycerate kinase	A0A5G2R4C4	[K].DCVGPEVEK.[A]	80	1.89	*
15	2-phospho-D-glycerate hydro-lyase	A0A4X1W8R1	[K].YINEFLAPALCTQK.[L]	233	0.76	**
16	4-Alpha-glucanotransferase	A0A287AXA8	[R].GVPALIENDHHMNCIR.[K]	283	1.41	*
17	Alpha-1,4 glucan phosphorylase	A0A4X1VBN9	[KR].TCAYTNHTVLPEALER.[W]	373	2.25	*
18	Serine/threonine-protein phosphatase	F1RNL4	[KR].HDLDLICR.[A]	246	2.10	**
		A0A4X1VTD3	[R].NVVTIFSAPNYCYR.[C]	266	1.98	**
19	Annexin	A0A5G2RBI3	[K].CLTEILASR.[T]	82	1.94	**
20	Calreticulin	A0A4X1T9R5	[K].HEQNIDCGGGYVK.[L]	71	1.44	*
21	Fibrillin-1	A0A4X1SK88	[K].GTCWQTIIDGR.[C]	853	1.58	*
22	Inosine-5′-monophosphate dehydrogenase	A0A4X1SXS6	[K].AQHGFCGIPITDTGR.[M]	140	1.48	*
23	Nicotinamide phosphoribosyltransferase	A0A5G2QUY8	[K].VYSYFECR.[E]	39	1.7	**
24	GTP-binding nuclear protein Ran	A0A5G2QZY6	[R].VCENIPIVLCGNK.[V]	126	1.67	*
25	ADP/ATP translocase	F1RZQ6	[R].KGADIMYTGTVDCWR.[K]	213	1.64	*
26	Ubiquitin carboxyl-terminal hydrolase	A0A4X1UWB5	[K].NEAIQAAHDAVAQEGQCR.[V]	152	1.87	**
27	Elongin C	A0A5G2QXY8	[K].TYGGCEGPDAMYVK.[L]	38	1.64	**
28	Mitsugumin-53	A0A5G2RAP2	[K].LQLQEACMR.[K]	118	1.74	*
			[K].YCLVTSR.[L]	216	1.73	*

Note: The protein name and accessions number of the identified peptide were recorded from www.uniprot.org/. FC indicated the fold change of specific Cys-SNO modification between PSE group and RFN group. * indicated $P < 0.05$ and ** indicated $P < 0.01$.

and the plasma membrane-cytoskeletal junction complex (Spurny et al., 2007). Recently, the degradation of plectin was found in pork LT muscle during 7 d of postmortem aging, suggesting a potential role in affecting meat quality of pork (Tian et al., 2019). In this study, we found that the Cys797 of plectin was modified by S-nitrosylation, and its expression in the PSE group was significantly higher than that in the RFN group. Spurny et al. (2007) found that the R5 domain of the plectin could undergo S-nitrosylation modification and a synergistic relationship was suggested between the S-nitrosylation of intermediate filament protein and S-nitrosylation of plectin (Horenberg et al., 2019).

In addition to the myofibrillar proteins, some of the sarcoplasmic proteins were also detected to be over-abundant in PSE group (Table 1). For example, the enzymes were related to glycogen metabolism and glycolysis included glyceraldehyde-3-phosphate dehydrogenase (GADPH), phosphoglycerate kinase (PGK), 4-α-glucanotransferase, 2-phospho-D-glycerate hydro-lyase, and 4-alpha-glucanotransferase. Some other proteins mainly belonged to phosphorylase (α-1,4-glucan phosphorylase, serine/threonine-protein phosphatase), transporters (GTP-binding nuclear protein Ran, and of ADP/ATP translocase), and proteases (elongin C and ubiquitin carboxyl-terminal hydrolase).

3.5. GO functional annotation of differentially modified proteins

The GO functional annotation of cellular component, biological process and molecular function was analyzed by using the data set of differential S-nitrosylated proteins between PSE and RFN meat. As shown in Fig. 4a, the differential proteins were mainly distributed in cytoskeletal and contractile fibers including myofibrils, contractile fiber, I band, sarcomere and supramolecular fiber. These proteins participated in muscular biological processes including the muscle system process, muscle structure and striated muscle cell development, muscle contraction and sarcomere organization. Accordingly, the molecular functions of those proteins were structural constituent of muscle, cytoskeletal protein binding, actinin binding and purine nucleoside binding. Likewise, previous studies have also shown that NO-induced nitrosylation could impact muscular biological processes such as muscle contraction and muscle structural composition by modifying myofibrillar protein and cytoskeletal protein (Bansbach and Guilford, 2016; Evangelista et al., 2010; Horenberg et al., 2019).

3.6. KEGG pathway and PPI analysis of differential S-nitrosylation-modified proteins

The enriched KEGG pathway for differential proteins of S-nitrosylation is shown in Fig. 4b. The top cellular processes were shown as tight junction, regulation of actin cytoskeleton, and necroptosis. The significant KEGG pathways for environment information processing were identified as HIF-1 signaling pathway, AMPK signaling pathway and TGF-beta signaling pathway. The enrichment of KEGG pathways which were involved in postmortem metabolism was glycolysis/glycogenesis. Coincidentally, those remarkable pathways were found in PPI network. Several co-expressed protein clusters were revealed and

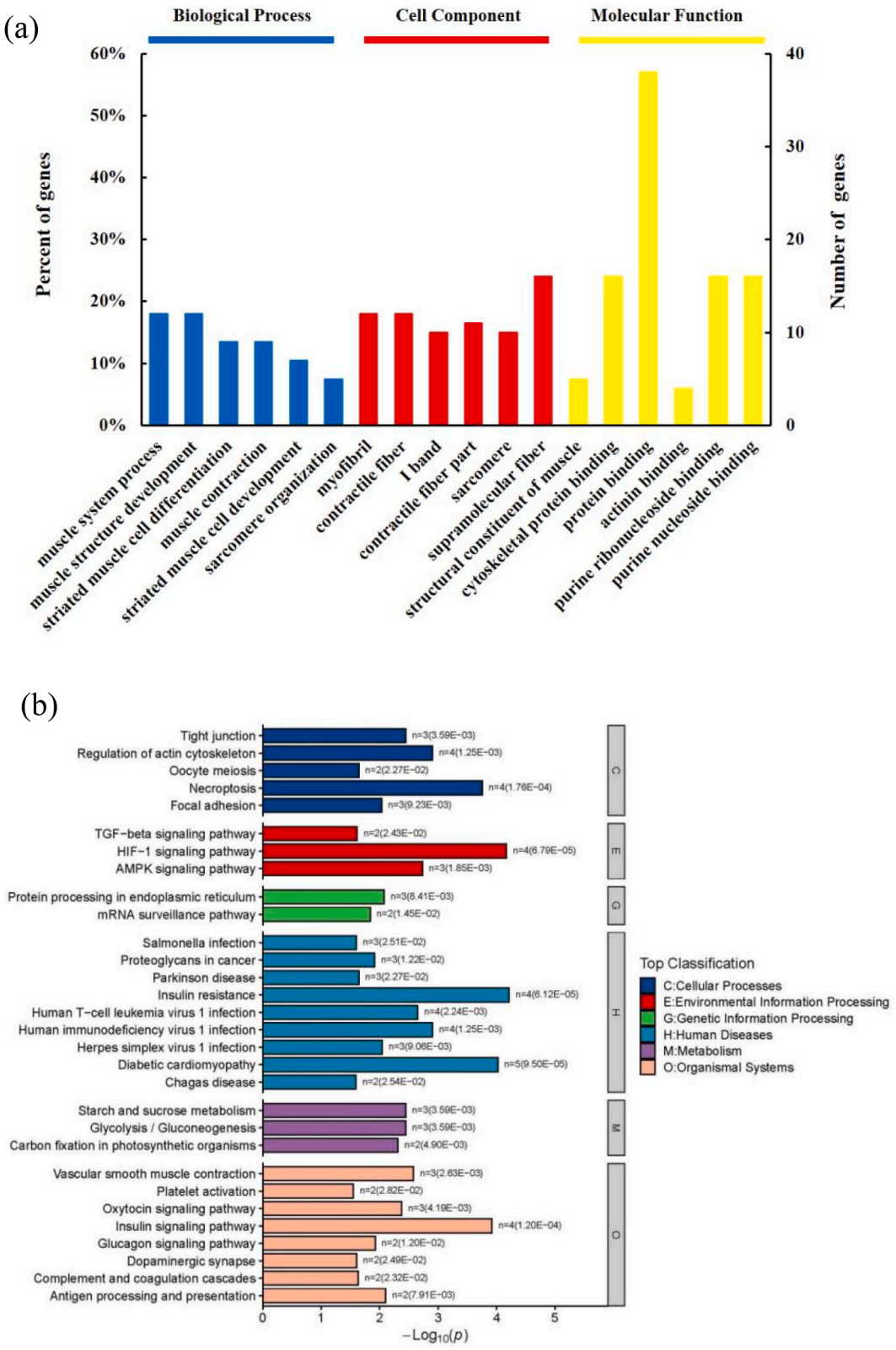

Fig. 4. GO functional classifications (a) and enrichment of KEGG pathway (b) by analyzing the differential proteins with S-nitrosylation modification between the PSE and RFN meat at 1 d of postmortem aging.

related to the HIF-1 signaling pathway, biosynthesis of amino acids, carbon metabolism, glycolysis/glycogenesis, muscle system processes, myofibril assembly, muscle cell development, striated muscle cell development and tight binding (Fig. 5). The genes corresponded with over-abundance SNO-modified proteins in PSE group such as PPP2CA, MYL6, LOC100523824, CSRP3, LDB3, SRL, SLMAP, FLNC, LMCD1 and TRIM72 was involved in the process of muscle system process, assembly of myofibrils and development of muscle cells. The tight binding process

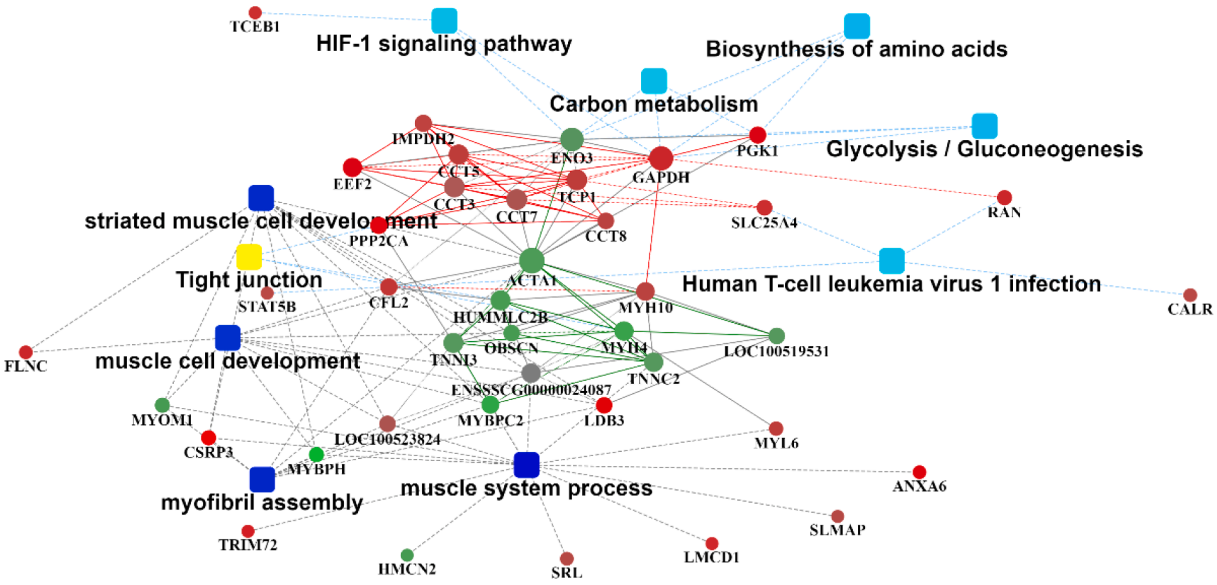

Fig. 5. Protein-protein interaction (PPI) network of the differentially modified proteins between the PSE and RFN meat at 1 d of postmortem aging.

included MYH4 and HUMMLC2B and PPP2CA. Moreover, the GAPDH and ENO3 were co-existed in glycolysis/glycogenesis and HIF-1 signaling pathway.

HIF-1 signaling pathway is activated in response to low oxygen concentration (Martínez-Ruiz & Lamas, 2004; Sha & Marshall, 2012), which is able to regulate genes involved in cell survival and glycolysis, thereby inhibiting apoptosis (Lambert, Roy, Robitaille, Richard, & Bonnet, 2010). It was reported that the expressions of glycolysis rate-limiting enzymes including glycogen phosphorylase (GP), phosphofructokinase (PFK), and pyruvate kinase (PK) in PSE meat were significantly higher than that in RFN meat, while the corresponding protein S-nitrosylation was lower (Wang et al., 2020). However, the current study showed that the S-nitrosylation of GAPDH and PGK in PSE meat was identified to be more expressed than that in RFN meat. The glycolytic enzymes are water-soluble proteins and shall be washed with low ionic buffer during the preparation of myofibrillar fraction of proteins. The existence of glycolytic enzymes in myofibrillar fraction of proteins in the present study was possibly due to that the lower pH in PSE meat might denature proteins and precipitate with myofribillar proteins during the extraction. On the other hand, those proteins may probably have the interactions with myofibrillar proteins as protein S-nitrosylation is able to change protein conformation, localization and protein–protein interaction (Hess et al., 2005).

Most importantly, the PPI analysis showed that the differentially modified proteins were involved in the muscle cell development and myofibril assembly. NO was originally known as an endothelium-derived relaxing factor to cause the relaxation of smooth muscle via NO/cGMP/PKG pathway (Bruckdorfer, 2005), until a direct effect of NO on the contractile apparatus of skeletal muscle was found (Horenberg et al., 2019). The chemical donor of free NO in skeletal muscle preparations led to the reduction of calcium ion sensitivity, ATP enzyme activity and shortening speed (Andrade, Reid, Allen, & Westerblad, 1998), which indicated that NO had a direct effect on myofibrillar protein in striated muscle (Horenberg et al., 2019). Moreover, studies have also shown that the S-nitrosylation modification could participate in the regulation of striated muscle through the regulation mechanism of myosin (Evangelista et al., 2010). Taking together, it is suggested that the S-nitrosylation of myofibrillar proteins detected in the current study can be regarded as a complementary pathway of NO in affecting meat quality and being involved in the process of muscle to meat conversion.

4. Conclusions

This paper explored the underlying mechanism of NO involved in postmortem aging via S-nitrosylation modification of myofibrillar proteins in PSE meat and RFN meat. It was found that the myofibrillar protein of PSE meat showed a higher degree of S-nitrosylation modification than that of RFN meat. The myofibrillar proteins including myosin, actin, actinin, nebulin, titin, troponin-I, filamin, plectin, microtubule-associated protein and PDZ and LIM domain protein were found to be S-nitrosylated and differentially expressed in PSE and RFN meat. The differential proteins were mainly distributed in the cytoskeleton, and participated in muscle system processes and myofibril assembly by exerting molecular functions of protein binding. In addition to glycolysis and energy metabolism, other biochemical processes related to meat quality were found such as the myofibril assembly, tight binding, and HIF-1 signaling pathway. Thus, the modification of myofibrillar protein by NO-induced S-nitrosylation can facilitate to understand NO-involved biochemical metabolism of postmortem muscle and explain the mechanism of PSE meat formation. The differential S-nitrosylated proteins with a high abundance in PSE group can be suggested a potential marker for meat grading in pork industry. On the other hand, molecular understanding of PSE pork might give practical implications in decreasing its occurrence and meeting consumers' demand for high quality pork meat. Further studies need to be further conducted on specific Cys-sites modification of myofibrillar proteins including myosin and actin on muscle contraction and meat quality during postmortem aging.

CRediT authorship contribution statement

Rui Liu: Conceptualization, Methodology, Software, Writing – original draft, Writing – review & editing. **Keyue Li:** Formal analysis, Data curation, Methodology, Investigation. **Guoyue Wu:** Writing – original draft, Investigation, Formal analysis. **Man Qin:** Data curation, Methodology, Investigation, Validation. **Hai Yu:** Data curation, Resources. **Mangang Wu:** Data curation, Methodology, Validation. **Qingfeng Ge:** Data curation, Methodology, Validation. **Shenglong Wu:** Resources. **Wenbin Bao:** Resources. **Wangang Zhang:** Supervision, Resources.

Declaration of Competing Interest

The authors declare that they have no known competing financial interests or personal relationships that could have appeared to influence the work reported in this paper.

Data availability

Data will be made available on request.

Acknowledgements

This work has been supported by Natural Science Foundation of Jiangsu Province (BK20190888), National Natural Science Foundation of China (No. 31901610), and Fellowship of China Postdoctoral Science Foundation (2020M671626). The technical support of Opening research of Jiangsu Key Laboratory of Animal genetic Breeding and Molecular Design (AGBMD2020) and Shanghai Bioprofile Biotechnology Co., Ltd. (Shanghai, China) are also acknowledged.

Appendix A. Supplementary data

Supplementary data to this article can be found online at https://doi.org/10.1016/j.foodchem.2022.133577.

References

Andrade, F. H., Reid, M. B., Allen, D. G., & Westerblad, H. (1998). Effect of nitric oxide on single skeletal muscle fibres from the mouse. *The Journal of Physiology, 509*(2), 577–586. https://doi.org/10.4152/pea.201405325

Bansbach, H. M., & Guilford, W. H. (2016). Actin nitrosylation and its effect on myosin driven motility. *AIMS Molecular Science, 3*(3), 426–438. https://doi.org/10.3934/molsci.2016.3.426

Barbut, S., Sosnicki, A. A., Lonergan, S. M., Knapp, T., Ciobanu, D. C., Gatcliffe, L. J., … Wilson, E. W. (2008). Progress in reducing the pale, soft and exudative (PSE) problem inpork and poultry meat. *Meat Science, 79*, 46–63. https://doi.org/10.1016/j.meatsci.2007.07.031

Bizzozero, O. A., & Zheng, J. (2009). Identification of major S-nitrosylated proteins in murine experimental autoimmune encephalomyelitis. *Journal of Neuroscience Research, 87*(13), 2881–2889. https://doi.org/10.1002/jnr.22113

Brannan, R. G., & Decker, E. A. (2002). Nitric oxide synthase activity in muscle foods. *Meat Science, 62*(2), 229–235. https://doi.org/10.1016/S0309-1740(01)00251-0

Bruckdorfer, R. (2005). The basics about nitric oxide. *Molecular Aspects of Medicine, 26*, 3–31. https://doi.org/10.1016/j.mam.2004.09.002

Chen, S. C., Huang, B., Liu, Y. C., Shyu, K. G., Lin, P. Y., & Wang, D. L. (2008). Acute hypoxia enhances proteins' S-nitrosylation in endothelial cells. *Biochemical and Biophysical Research Communications, 377*(4), 1274–1278. https://doi.org/10.1016/j.bbrc.2008.10.144

Chmiel, M., Slowinski, M., & Janakowski, S. (2014). The quality evaluation of RFN and PSE pork longissimus lumborum muscle considering its microstructure. *Annals of Animal Science, 14*(3), 737. https://doi.org/10.2478/aoas-2014-0035

Cottrell, J., Ponnampalam, E., Dunshea, F., & Warner, R. (2015). Effects of infusing nitric oxide donors and inhibitors on plasma metabolites, muscle lactate production and meat quality in lambs fed a high quality roughage-based diet. *Meat Science, 105*, 8–15. https://doi.org/10.1016/j.meatsci.2015.02.007

Cottrell, J. J., McDonagh, M., Dunshea, F., & Warner, R. (2008). Inhibition of nitric oxide release pre-slaughter increases post-mortem glycolysis and improves tenderness in ovine muscles. *Meat Science, 80*(2), 511–521. https://doi.org/10.1016/j.meatsci.2008.02.002

Evangelista, A. M., Rao, V. S., Filo, A. R., Marozkina, N. V., Doctor, A., Jones, D. R., … Guilford, W. H. (2010). Direct regulation of striated muscle myosins by nitric oxide and endogenous nitrosothiols. *PloS One, 5*(6), e11209.

Figueiredo-Freitas, C., Dulce, R. A., Foster, M. W., Liang, J., Yamashita, A. M., Lima-Rosa, F. L., … Nogueira, L. (2015). S-nitrosylation of sarcomeric proteins depresses myofilament Ca^{2+} sensitivity in intact cardiomyocytes. *Antioxidants & Redox Signaling, 23*(13), 1017–1034. https://doi.org/10.1089/ars.2015.6275

Hartman, M. A., & Spudich, J. A. (2012). The myosin superfamily at a glance. *Journal of Cell Science, 125*(7), 1627–1632. https://doi.org/10.1242/jcs.094300

Hess, D. T., Matsumoto, A., Kim, S.-O., Marshall, H. E., & Stamler, J. S. (2005). Protein S-nitrosylation: Purview and parameters. *Nature Reviews Molecular Cell Biology, 6*(2), 150–166. https://doi.org/10.1038/nrm1569

Horenberg, A. L., Houghton, A. M., Pandey, S., Seshadri, V., & Guilford, W. H. (2019). S-nitrosylation of cytoskeletal proteins. *Cytoskeleton, 76*(3), 243–253. https://doi.org/10.1002/cm.21520

Huff-Lonergan, E., & Lonergan, S. M. (2005). Mechanism of water-holding capacity of meat: The role of postmortem biochemical and structural changes. *Meat Science, 71*, 194–204. https://doi.org/10.1016/j.meatsci.2005.04.022

Huff-Lonergan, E., Zhang, W. G., & Lonergan, S. M. (2010). Biochemistry of postmortem muscle-Lessons on mechanisms of meat tenderization. *Meat Science, 86*, 184–195. https://doi.org/10.1016/j.meatsci.2010.05.004

Hwang, I. H., Park, B. Y., Kim, J. H., Cho, S. H., & Lee, J. M. (2005). Assessment of postmortem proteolysis by gel-based proteome analysis and its relationship to meat quality traits in pig longissimus. *Meat Science, 69*(1), 79–91. https://doi.org/10.1016/j.meatsci.2004.06.019

Karamucki, T., Jakubowska, M., Rybarczyk, A., & Gardzielewska, J. (2013). The influence of myoglobin on the colour of minced pork loin. *Meat Science, 94*(2), 234–238. https://doi.org/10.1016/j.meatsci.2013.01.014

Lambert, C. M., Roy, M., Robitaille, G. A., Richard, D. E., & Bonnet, S. (2010). HIF-1 inhibition decreases systemic vascular remodelling diseases by promoting apoptosis through a hexokinase 2-dependent mechanism. *Cardiovascular Research, 88*(1), 196–204. https://doi.org/10.1093/cvr/cvq152

Lametsch, R., Karlsson, A., Rosenvold, K., Andersen, H. J., Roepstorff, P., & Bendixen, E. (2003). Postmortem proteome changes of porcine muscle related to tenderness. *Journal of Agricultural and Food Chemistry, 51*(24), 6992–6997. https://doi.org/10.1021/jf034083p

Lana, A., & Zolla, L. (2016). Proteolysis in meat tenderization from the point of view of each single protein: A proteomic perspective. *Journal of Proteomics, 147*, 85–97. https://doi.org/10.1016/j.jprot.2016.02.011

Linke, W. A., & Hamdani, N. (2014). Gigantic business: Titin properties and function through thick and thin. *Circulation Research, 114*(6), 1052–1068. https://doi.org/10.1161/CIRCRESAHA.114.301286

Liu, R., Warner, R. D., Zhou, G. H., & Zhang, W. G. (2018a). Contribution of nitric oxide and protein S-nitrosylation to variation in fresh meat quality. *Meat Science, 144*, 135–148. https://doi.org/10.1016/j.meatsci.2018.04.027

Liu, R., Fu, Q. Q., Lonergan, S., Huff-Lonergan, E., Xing, L. J., Zhang, L. L., … Zhang, W. G. (2018b). Identification of S-nitrosylated proteins in postmortem pork muscle using modified biotin switch method coupled with isobaric tags. *Meat Science, 145*, 431–439. https://doi.org/10.1016/j.meatsci.2018.07.027

Liu, R., Li, Y. P., Zhang, W. G., Fu, Q. Q., Liu, N., & Zhou, G. H. (2015). Activity and expression of nitric oxide synthase in pork skeletal muscles. *Meat Science, 99*, 25–31. https://doi.org/10.1016/j.meatsci.2014.08.010

Martínez-Ruiz, A., & Lamas, S. (2004). S-nitrosylation: A potential new paradigm in signal transduction. *Cardiovascular Research, 62*(1), 43–52. https://doi.org/10.1016/j.cardiores.2004.01.013

Mayans, O., Wuerges, J., Canela, S., Gautel, M., & Wilmanns, M. (2001). Structural evidence for a possible role of reversible disulphide bridge formation in the elasticity of the muscle protein titin. *Structure, 9*(4), 331–340. https://doi.org/10.1016/S0969-2126(01)00591-3

Picard, B., Gagaoua, M., & Hollung, K. (2017). Gene and protein expression as a tool to explain/predict meat (and fish) quality. *New Aspects of Meat Quality, 321–354*. https://doi.org/10.1016/B978-0-08-100593-4.00013-8

Sha, Y., & Marshall, H. E. (2012). S-nitrosylation in the regulation of gene transcription. *Biochimica et Biophysica Acta (BBA)-General Subjects, 1820*(6), 701–711. https://doi.org/10.1016/j.bbagen.2011.05.008

Spurny, R., Abdoulrahman, K., Janda, L., Ruönzler, D., Koöhler, G., Castañón, M. J., & Wiche, G. (2007). Oxidation and nitrosylation of cysteines proximal to the intermediate filament (IF)-binding site of plectin: Effects on structure and vimentin binding and involvement in IF collapse. *Journal of Biological Chemistry, 282*(11), 8175–8187. https://doi.org/10.1074/jbc.M608473200

Stamler, J. S., & Meissner, G. J. (2001). Physiology of nitric oxide in skeletal muscle. *Physiological Reviews, 81*(1), 209–237. https://doi.org/10.1152/physrev.2001.81.1.209

Su, D., Shukla, A. K., Chen, B., Kim, J. S., Nakayasu, E., Qu, Y., … Monroe, M. E. (2013). Quantitative site-specific reactivity profiling of S-nitrosylation in mouse skeletal muscle using cysteinyl peptide enrichment coupled with mass spectrometry. *Free Radical Biology and Medicine, 57*, 68–78. https://doi.org/10.1016/j.freeradbiomed.2012.12.010

Tian, X. N., Wang, Y. Y., Fan, X. Q., Shi, Y. W., Zhang, W. G., Hou, Q., … Zhou, G. H. (2019). Expression of pork plectin during postmortem aging. *Journal of Agricultural and Food Chemistry, 67*(42), 11718–11727. https://doi.org/10.1021/acs.jafc.9b03040

Wang, Y., Hu, Y., Li, Y. K., Li, R., Pan, D. M., Fang, H. M., … Zhou, C. L. (2021). Individual effects of L-arginine or L-lysine on stability of pork or chicken emulsion sausages with partial replacement of porcine backfat by soybean oil. *International Journal of Food Science & Technology, 56*(12), 6742–6751. https://doi.org/10.1111/ijfs.15365

Wang, Y. Y., Liu, R., Hou, Q., Tian, X. N., Fan, X. Q., Zhang, W. G., & Zhou, G. H. (2020). Comparison of activity, expression, and S-nitrosylation of glycolytic enzymes between pale, soft, and exudative and red, firm, and non-exudative pork during post-mortem aging. *Food Chemistry, 314*, Article 126203. https://doi.org/10.1016/j.foodchem.2020.126203

Wang, Y. Y., Liu, R., Tian, X. N., Fan, X. Q., Shi, Y. W., Zhang, W. G., … Zhou, G. H. (2019). Comparison of activity, expression, and S-nitrosylation of calcium transfer proteins between pale, soft, and exudative and red, firm, and non-exudative Pork during post-mortem aging. *Journal of Agricultural and Food Chemistry, 67*(11), 3242–3248. https://doi.org/10.1021/acs.jafc.8b06448

Warner, R. D., Kauffman, R. G., & Greaser, M. L. (1997). Muscle protein changes post mortem in relation to pork quality traits. *Meat Science, 45*(3), 339–352. https://doi.org/10.1016/S0309-1740(96)00116-7

Woolner, S., & Bement, W. M. (2009). Unconventional myosins acting unconventionally. *Trends in Cell Biology, 19*(6), 245–252. https://doi.org/10.1016/j.tcb.2009.03.003

Zhu, Q. N., Xing, L. J., Hou, Q., Liu, R., & Zhang, W. G. (2021). Proteomics identification of differential S-nitrosylated proteins between the beef with intermediate and high

ultimate pH using isobaric iodoTMT switch assay. *Meat Science, 172*, Article 108321. https://doi.org/10.1016/j.meatsci.2020.108321